Equilibrium Evolution in the ZaP Flow Z-Pinch

U. Shumlak, C.S. Adams, R.P. Golingo, D.J. Den Hartog, S.L. Jackson, S. D. Knecht, K. A. Munson, B.A. Nelson, ZaP Team

Aerospace & Energetics Research Program, University of Washington, Seattle, WA, USA

e-mail contact of main author: shumlak@aa.washington.edu

Abstract. The ZaP Flow Z-pinch experiment at the University of Washington investigates the innovative plasma confinement concept of using sheared flows to stabilize an otherwise unstable configuration. The stabilizing effect of a sheared axial flow on the m = 1 kink instability in Z-pinches has been studied using linearized, ideal MHD theory to reveal that a sheared axial flow stabilizes the kink mode when the shear exceeds a threshold. The ZaP experiment generates an axially flowing Z-pinch that is 1 m long with a 1 cm radius with a coaxial accelerator coupled to a pinch assembly chamber. Magnetic probes measure the fluctuation levels of the azimuthal modes m = 1, 2, and 3. After assembly the plasma is magnetically confined for an extended quiescent period where the mode activity is significantly reduced. Time-resolved Doppler shifts of plasma impurity lines are measured along 20 chords to determine the plasma axial velocity profiles showing a large, but sub-Alfvenic, sheared flow during the quiescent period and low shear profiles during periods of high mode activity. The plasma has a sheared axial flow that exceeds the theoretical threshold for stability during the quiescent period and is lower than the threshold during periods of high mode activity. The sheared flow profile is coincident with a plasma quiescent period where magnetic mode fluctuations are low. The value of the velocity shear satisfies the theoretical threshold for stability during the quiescent period and does not satisfy the threshold during high mode activity. Multichord and holographic interferometers measure a Z-pinch plasma with a peaked radial profile during the quiescent period. Internal magnetic fields have been recently determined by measuring the Zeeman splitting of impurity carbon emission. The measurements are consistent with a well-confined pinch plasma.

1. Introduction

The ZaP Flow Z-pinch experiment at the University of Washington investigates the concept of using sheared flows to stabilize an otherwise unstable plasma configuration. The stabilizing effect of a sheared axial flow on the $m = 1$ kink instability in Z-pinches has been studied numerically using linearized ideal MHD theory. The principal result reveals that a
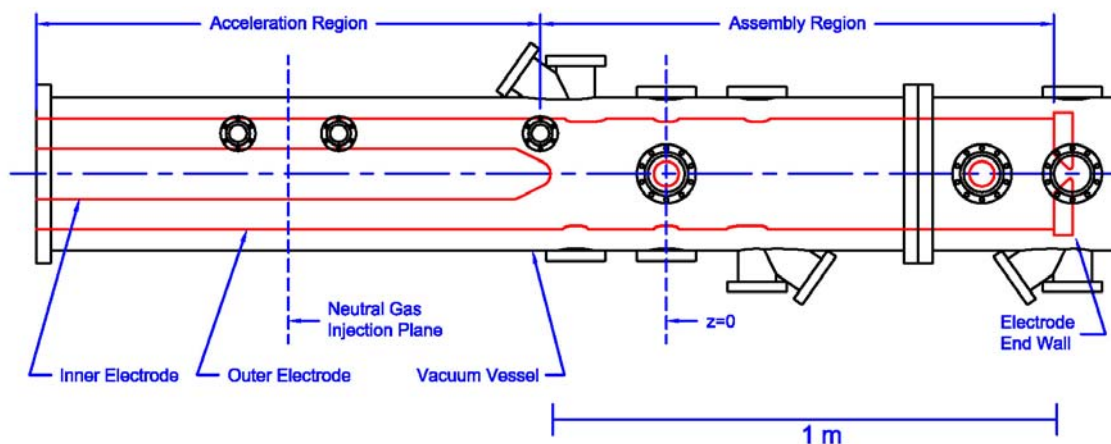

FIG. 1. Side view drawing of the ZaP Flow Z-Pinch experiment identifying the relevant features. The acceleration and assembly regions are identified. The ports at z = 0 are used by the holographic interferometer and the spectrometer used for Zeeman splitting measurements. A 1 m scale is included for reference.

sheared axial flow stabilizes the kink mode when the shear exceeds a threshold value, $dV_z/dr > 0.1$ kV_A.[1] Nonlinear simulations support the stabilizing effect. Previous experiments have generated Z-pinch plasmas that exist for times longer than theoretically predicted by static plasma theory.[2,3] These experiments have generated Z-pinch plasmas which inherently contain an axial plasma flow. This paper describes the evolution of the equilibrium based on experimental measurements with a holographic interferometer and Zeeman splitting of impurity line radiation.

2. ZaP Flow Z-Pinch Experiment

The ZaP Flow Z-pinch experiment at the University of Washington initiates a plasma with a 1 m long coaxial accelerator which has a 20 cm diameter outer electrode and a 10 cm diameter inner electrode. Neutral gas, typically hydrogen, is injected with fast gas puff valves into the midplane annulus of the coaxial accelerator. An electrical potential of $5 - 9$ kV is applied to the accelerator to breakdown the neutral gas, creating a plasma. The plasma is accelerated to a large axial velocity by a Lorentz force, exits the accelerator, and forms a Z-pinch plasma 1 m in length and 1 cm in radius. Current in the accelerator continues to accelerate plasma into the Z-pinch assembly replacing plasma as it exits the Z-pinch. Inertia maintains the axial flow within the Z-pinch plasma column. The plasma current is supplied by a 17.5 kJ capacitor bank configured as a pulse-forming network. The peak current is 150 - 200 kA with a rise time of 25 μs, a flat-top of 35 μs, and a fall time of 40 μs. A machine drawing of the experiment is shown in Fig. 1 which identifies the relevant hardware features. Data presented here are primarily from the r-θ plane of the Z-pinch defined at $z = 0$. (The Z-pinch extends from the end of the accelerator at $z = -25$ cm to the electrode end wall $z = 75$ cm.)

Diagnostics on the ZaP experiment are designed to measure the plasma flow profile and the stability of the pinch, as well as the plasma equilibrium parameters. Plasma stability is
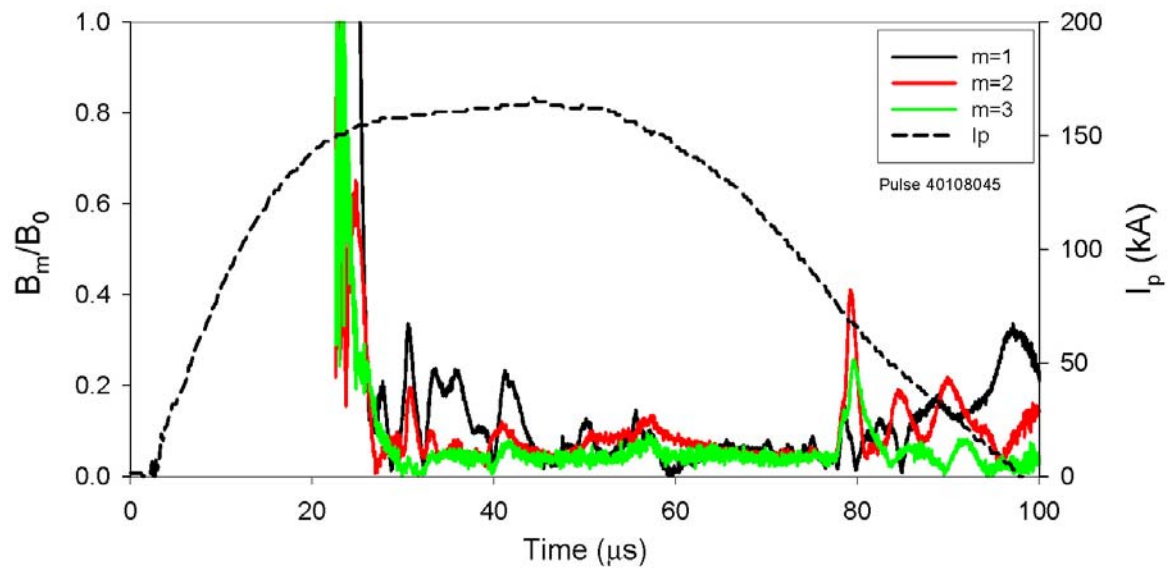

FIG. 2. *Time evolution of the Fourier components of the magnetic field fluctuations at z = 0 for the m = 1,2,3 modes. The values are normalized to the average magnetic field value. A quiescent period is evident from 42 to 79 μs which defines τ = 0 to 1 for this pulse. The evolution of the plasma current is included for reference.*

diagnosed with an azimuthal array of eight magnetic probes that measures the plasma's magnetic structure. Data from these probes are Fourier analyzed to determine the time-dependent evolution of the low order azimuthal modes (m = 1, 2, 3), as shown in Fig. 2. Large magnetic fluctuations occur during pinch assembly, after which the amplitude and frequency of the magnetic fluctuations diminish. This stable behavior continues for 35 - 45 µs and defines the quiescent period. A 37 µs quiescent period is seen in Fig. 2. At the end of the quiescent period, the fluctuation levels again change character, increase in magnitude and frequency, and remain until the end of the plasma pulse. Time is normalized to the quiescent period to allow comparison between pulses. $\tau = 0$ is defined as the beginning and $\tau = 1$ is defined as the end of the quiescent period. The quiescent period is coincident with a sheared axial flow that satisfies the theoretical threshold. [1,4,5,6,7]

3. Density Analysis

The evolution of plasma equilibrium is studied. A holographic interferometer provides high resolution electron number density profile information at a single time. The interferometer uses a pulsed ruby laser in a double-pass or single-pass configuration. Holographic film is double exposed, first without plasma present and then with plasma present and a tilting mirror activated. The tilting mirror introduces vertical reference fringes onto the hologram. Deflection away from vertical is proportional to the chord-integrated density. A sample holographic interferogram is shown in Fig. 3. The chord-integrated density from the interferograms is deconvolved to determine density profiles.[8] During the quiescent period, the density profile shows a discrete plasma pinch where density peaks on axis and is reduced to a small value at the edge. Figure 4 shows the density profile in a helium plasma obtained at $\tau = 0.65$. Later in the quiescent period, the density profile is reduced but a discrete plasma pinch is still evident, as shown in Fig. 5. After the quiescent period, the density profile shows a background density that is mostly low and uniform. The density measurements agree with those from a two-chord He-Ne interferometer.

The density profiles are analyzed using the magnetic field measured at the outer electrode and the input power to compute equilibrium temperature and magnetic field profiles. The input power is measured at the electrical feeds to the electrodes and is the upper limit. It is assumed to be uniformly deposited in the pinch plasma. The plasma temperature is assumed to be zero
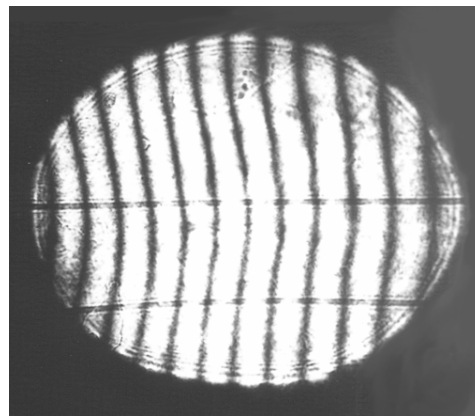

FIG. 3. Holographic interferogram showing fringes deflected from vertical indicating plasma density. The machine axis is horizontal. The two thin horizontal lines are produced by reference wires spaced 1 cm apart. (Pulse 210029011)
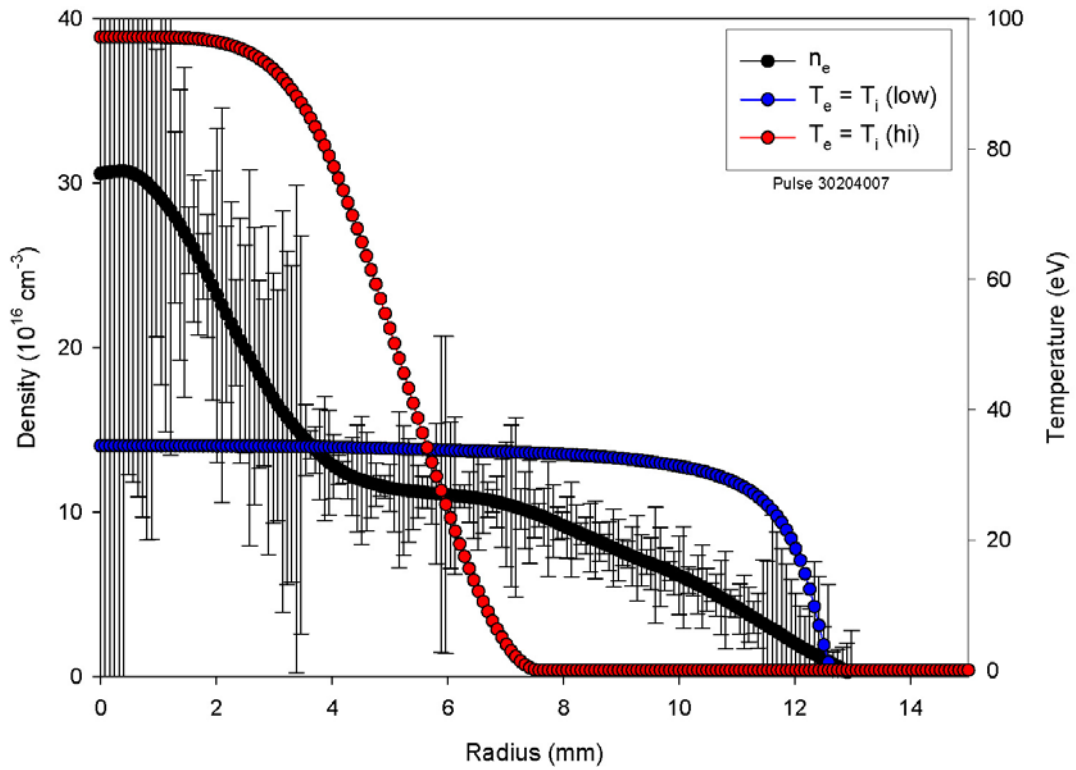
FIG. 4. Deconvolved density profile in a helium plasma at τ = 0.65. A discrete plasma pinch is evident with a radius of approximately 8 mm. Ion temperature profiles are calculated from radial thermal conduction and equilibrium force balance.
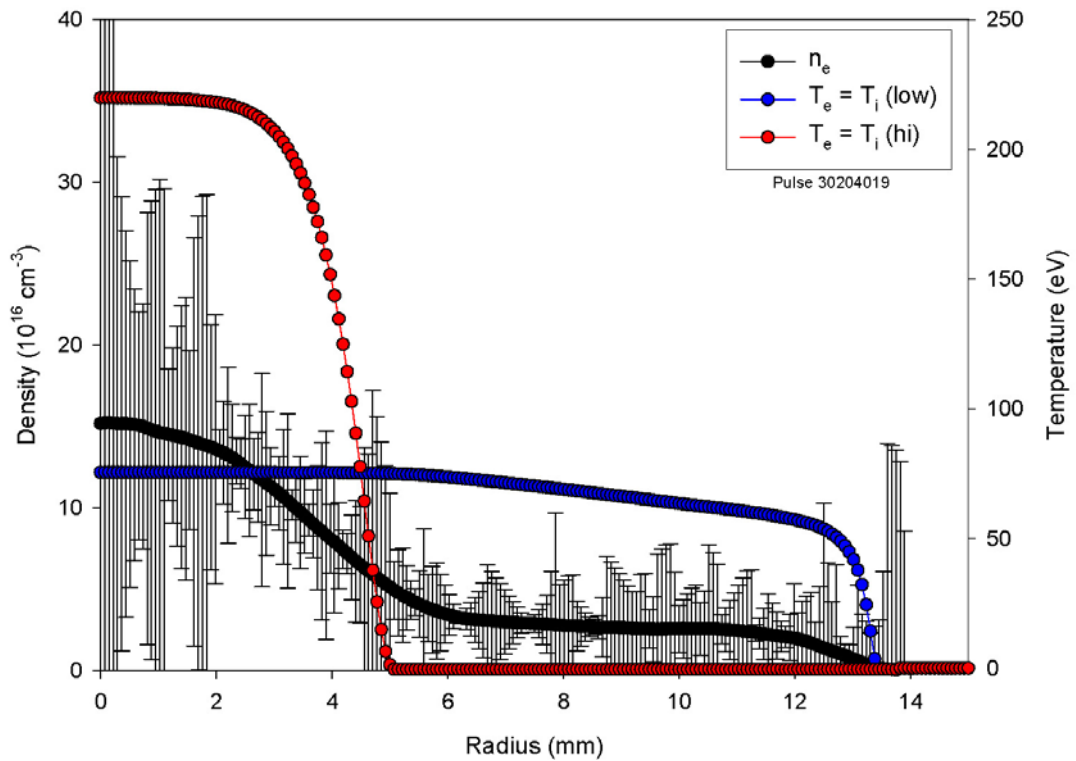
FIG. 5. Deconvolved density profile in a helium plasma at τ = 0.73. Pinch radius has decreased to approximately 6 mm. Ion temperature has increased.

The perpendicular radial thermal conductivities are given by Braginskii[9] as

$$k_{\perp e} = 4.7 \frac{n_e T_e}{m_e \omega_{ce}^2 \tau_e} \quad \text{and} \quad k_{\perp i} = 2 \frac{n_i T_i}{m_i \omega_{ci}^2 \tau_i},\tag{1}$$

with appropriate limits at the axis where the magnetic field vanishes. The input power is transported by radial heat conduction. Therefore, the radial thermal conduction is given as a balance between the input power and the radial heat flux.

$$\dot{q} = -\frac{1}{r} \frac{d}{dr} \left[r \left(k_{\perp e} T_e + k_{\perp i} T_i \right) \right]\tag{2}$$

The radial force balance is expressed as

$$\frac{B_\theta}{\mu_o r} \frac{d\left(r B_\theta\right)}{dr} = -\frac{d}{dr}\left(n_e T_e + n_i T_i\right).\tag{3}$$

Equations (1) - (3) are solved with a measured magnetic field of 0.16 T at the outer electrode and an input power of 400 MW. The resulting ion temperature profiles are shown in Figs. 4 and 5 as the red curves. $T_e = T_i$ is assumed. Since the red curves represent upper limits, the calculations are repeated assuming a reduced input power to determine lower limits which are also shown in the figures. The analysis also computes the magnetic field profiles corresponding to the density and temperature profiles. The magnetic field peaks at 2.3 T and 1.3 T for the data in Fig. 4 for the high and low temperature profiles, respectively. The magnetic field peaks at 3.2 T and 1.4 T for the data in Fig. 5 for the high and low temperature profiles, respectively.

4. Internal Magnetic Fields

Surface probes in the outer electrode measure external magnetic fields. Zeeman splitting is used to measure internal magnetic fields.[10] Impurity emission of the C IV doublet at 580.1 and 581.2 nm is collected perpendicular to the plasma axis along 10 pairs of parallel chords through the pinch plasma using an imaging spectrometer with an intensified CCD camera (ICCD) operated with a 500 ns gate during the quiescent period. A component of the azimuthal magnetic field is parallel to the viewing direction, and, therefore, the Zeeman Effect causes a splitting of the circularly polarized σ components of the emission. The circularly polarized light is sent through a quarter-wave plate and then through linear polarizers to distinguish the left-hand polarized (LHP) and right-hand polarized (RHP) light. Each of the 10 pairs of collected light is sent through a quarter-wave plate to convert the circularly polarized light into linearly polarized light. The LHP and RHP light becomes vertically and horizontally linearly polarized light which is separated by using linear polarizers oriented perpendicularly. This technique allows a measurement of the Zeeman splitting even when the separation of the spectral components is small compared to their broadening.

Sample raw data are presented in Fig. 6 for 3 of the 10 pairs of parallel chords. Shown are the shifts of the LHP and RHP light from the nominal wavelengths for C IV doublet at 3 impact parameters. The data collected at an impact parameter of 0.0 mm corresponding to the geometric center of the device show little shift and therefore low magnetic field. At the -11.3 mm impact parameter, the RHP is shifted to the right and the LHP is shifted to the left. The shifts are consistent with a large magnetic field aligned with the viewing direction. At the 11.3 mm impact parameter, the shifts are reversed. The RHP is shifted to the left and the LHP is shifted to the right. The shifts are consistent with a large magnetic field aligned oppositely with the viewing direction.
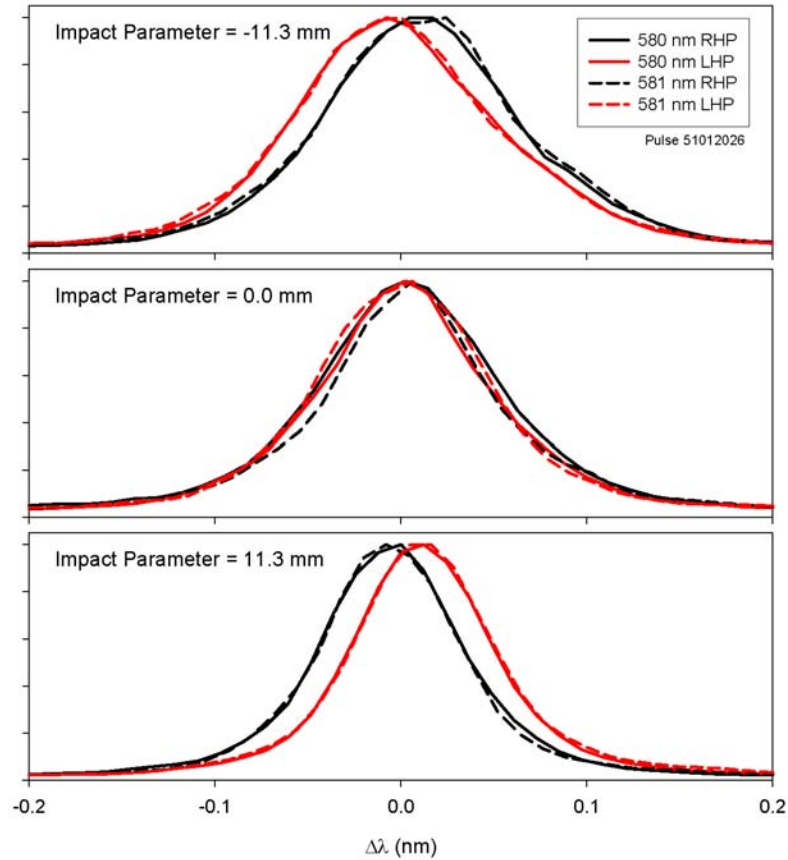
FIG. 6. Raw spectral data showing the displacement of the right-hand polarized (RHP) and left-hand polarized (LHP) light from the C IV doublet. The direction and magnitude of the shifts of the RHP and LHP are consistent with a Z-pinch magnetic field centered at the geometric center.

The data are deconvolved to determine magnetic field profiles as functions of radius. Figure 7 shows the results from a collection of several pulses as indicated by the different symbol colors. The measurements presented in Fig. 7 are produced by injecting methane gas and using lower capacitor bank energy. Typical ZaP plasmas burn through C IV, and signal levels become too low to accurately measure the Zeeman splitting. The variation of the profiles is caused by pulse-to-pulse variation in the location of the C IV emission. The emission is typically occurs from an annular region that moves outward throughout the plasma lifetime. Data collected early in the pulse corresponds to light emission from radii inside the pinch radius, and therefore the magnetic fields are lower. Similarly, data collected late in the pulse corresponds to light emission from radii outside the pinch radius, and again the magnetic fields are lower. Therefore, the magnetic field values measured with this technique provide a lower bound on the magnetic field profile. The magnetic field values in Fig. 7 are compared to an inverse radius fit to the value measured at the outer electrode. The data indicate a characteristic pinch radius of approximately 10 mm and fits the inverse radius envelope for larger radii indicating the plasma current is contained inside the pinch radius. The magnetic field profile is similar to those calculated from the density profiles in the previous section.
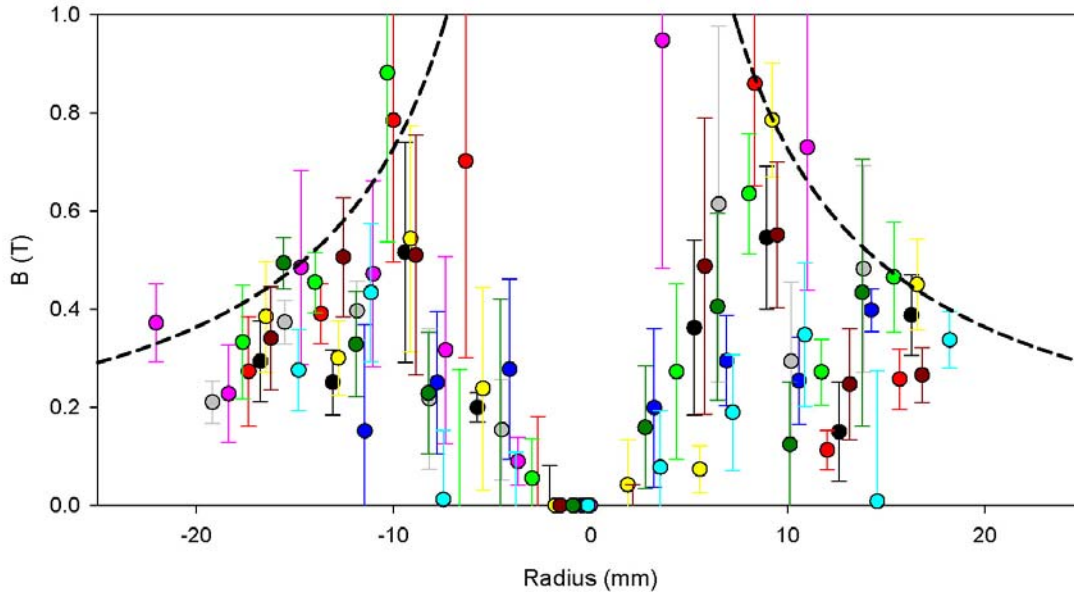
*FIG. 7. Internal magnetic field measured by Zeeman splitting of C IV line for several pulses.
Each pulse has the same color data symbol. Dashed line shows inverse radius fit from outer
electrode surface probe.*

5. Discussion

The ZaP project is producing Z-pinch plasmas that exhibit gross stability during a quiescent
period, consistent with flow stabilization theory. Analyzed density profiles show high
temperature and magnetic field profiles during the quiescent period. Internal magnetic field
measurements are consistent with the analyzed profiles.

If it is assumed that velocity shear is playing the critical role of providing stability for the
otherwise unstable Z-pinch, then two possible mechanisms that limit the lifetime of the
plasma confinement are decay of plasma current and loss of plasma flow or flow shear. These
two mechanisms may not be completely independent. Previous experiments conducted with
different plenum pressures in the puff valves appear to discount the decay of plasma current
as the lifetime limiting mechanism.[11] Loss of plasma flow is a more likely mechanism that
limits the plasma lifetime. The loss of plasma flow may result from stagnation on the
electrode end wall, shown in Fig. 1. A plasma exhaust hole is installed to reduce flow
stagnation. Experimental measurements indicate a decrease of plasma acceleration in the
acceleration region that is approximately coincident with the end of the quiescent period in
the Z-pinch plasma.[6] Specifically, the azimuthal magnetic field values measured at several
axial locations converge to the same value indicating a decrease of radial current in the
acceleration region. Plasma density in the acceleration region is also observed to decrease
during these same experiments.[6] While not conclusive, the experimental results suggest the
loss of plasma flow may be caused by a depletion of the injected neutral gas. The
experimental results presented here further support this conjecture. The results presented in
Fig. 5 show a reduced plasma density later in the quiescent period. After the quiescent period
the density drops to zero (within the accuracy of the measurement), though this may also be
explained by the instabilities. Experiments are on-going to further investigate the dependence
of the plasma lifetime on injected neutral gas. Future experimental modifications include

additional gas puffing capacity to approach a quasi steady-state operation of the ZaP Flow Z-Pinch experiment. True steady state is not likely to be possible with gas puff valves; however, using plasma injectors may be feasible.

The internal measurements of density profiles and magnetic field profiles demonstrate the flow Z-pinch establishes an equilibrium described by a radial force balance. The analyzed profiles of the temperature and magnetic field are consistent with other measurements – ion Doppler spectral broadening for ion temperature and Zeeman splitting for magnetic field. The data indicate a high-temperature, high-density plasma is sustained throughout an extended quiescent period that is many times greater than expected lifetime for a static Z-pinch.

Z-pinch plasmas have high plasma densities and can reach high plasma temperatures. However, plasma stability has limited their usefulness as a magnetic fusion configuration. The flow Z-pinch may provide a unique solution if the Z-pinch can be stabilized with a sheared plasma flow and the equilibrium state can be sustained with a steady, or even quasi steady, flow. A flow-stabilized Z-pinch has many important implications for a simple reactor design and other magnetic confinement concepts. Furthermore, the stabilizing effect of a sheared flow may be applicable to other magnetic confinement concepts perhaps reducing the engineering complexity and thereby the overall cost.

[1]   U. Shumlak and C.W. Hartman, Phys. Rev. Lett. **75,** 3285 (1995)
[2]   A.A. Newton, J. Marshall, and R. L. Morse, "Proc. 3rd Euro. Conf. on Controlled Fusion Plasma Phys.," Utrecht, 119 (1969)
[3]   V.G. Belan, S. P. Zolotarev, V. F. Levahov, V. S. Mainashev, A. I. Morozov, V. L. Podkovyrov, and Yu. V. Skvortsov, Sov. J. Plasma Physics **16,** 96 (1990)
[4]   R.P. Golingo and U. Shumlak, Rev. Sci. Instrum. **74** (4), 2332 (2003)
[5]   U. Shumlak, R. P. Golingo, B. A. Nelson, and D. J. Den Hartog, Phys. Rev. Lett. **87,** 205005 (2001)
[6]   U. Shumlak, B. A. Nelson, R. P. Golingo, S. L. Jackson, E. A. Crawford, and D. J. Den Hartog, Phys. Plasmas **10** (5), 1683 (2003)
[7]   R.P. Golingo, U. Shumlak, and B.A. Nelson, Phys. Plasmas **12**, 62505 (2005)
[8]   S.L. Jackson and U. Shumlak, Rev. Sci. Instrum. **77**, 083502 (2006)
[9]   S.I. Braginskii, Reviews of Plasma Physics **1,** 205 (1965)
[10]   T. Shikama, S. Kado, H. Zushi, A. Iwamae, and S. Tanaka, Phys. Plasmas **11** (10), 4701 (2004)
[11]   U. Shumlak, C. S. Adams, R. P. Golingo, S. L. Jackson, B. A. Nelson, and T. L. Shreve, IAEA-CN-116/ICP6-47 (2004)